Accepted Manuscript

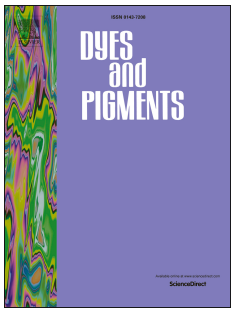

A study on the fluorescence property of the perylene derivatives with methoxy groups

Jeong Yun Kim, Sung Wun Woo, Jin Woong Namgoong, Jae Pil Kim

PII: S0143-7208(17)31519-X

DOI: 10.1016/j.dyepig.2017.08.060

Reference: DYPI 6222

To appear in: *Dyes and Pigments*

Received Date: 11 July 2017

Revised Date: 25 August 2017

Accepted Date: 25 August 2017

Please cite this article as: Kim JY, Woo SW, Namgoong JW, Kim JP, A study on the fluorescence property of the perylene derivatives with methoxy groups, *Dyes and Pigments* (2017), doi: 10.1016/j.dyepig.2017.08.060.

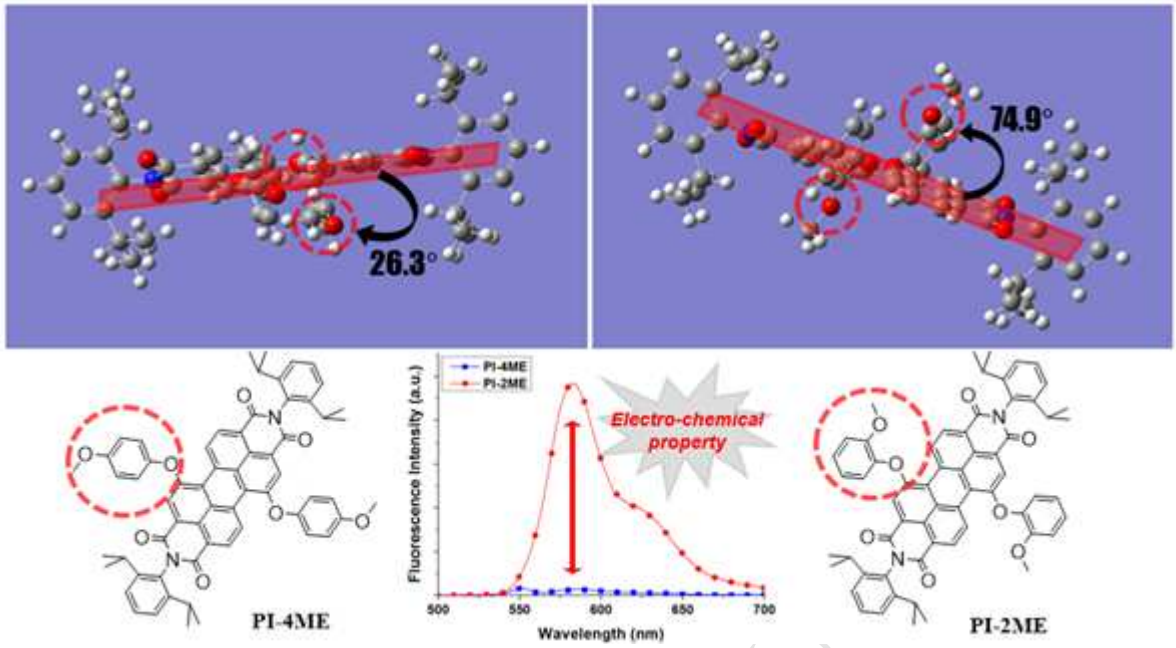

Graphical abstract

A study on the fluorescence property of the perylene derivatives with methoxy groups

Jeong Yun Kim [a], Sung Wun Woo [a], Jin Woong Namgoong [a], Jae Pil Kim [a,*]

a. Lab. of Organic Photo-functional Materials, Department of Materials Science and Engineering, Seoul National University, Seoul 08826, Republic of Korea

[*] Corresponding author. Tel.: +82 2 880 7187; fax: +82 2 880 7238

E-mail address: jaepil@snu.ac.kr (J. P. Kim)

Abstract

Perylene-based dyes with methoxy groups at various positions were synthesized to understand the effect of the methoxy groups on the fluorescence quenching. Additionally, perylene-based dyes with ethyl groups in place of the methoxy groups were also synthesized to serve as control. Absorption and fluorescence properties of the dyes were measured, and then, density functional theory (DFT) and time-dependent density functional theory (TD-DFT) simulations were conducted. The methoxy groups of terminal-substituents had a lesser effect on fluorescence quenching than the methoxy groups of bay-substituents. Moreover, only the methoxy groups at the para-position of the bay-substituents strongly affected on fluorescence quenching. These results showed that the fluorescence of the dyes are influenced by the electron donating effect of the methoxy groups when the methoxy groups are involved in the main conjugation systems of the dyes.

Keywords

Perylene, Fluorescence, Fluorescence quenching, Methoxy, Electron donating effect, TD-DFT

1. Introduction

Perylene-based dyes generally show superior thermal stability and optical properties owing to the planarity of their molecular structures [1-5]. Because of these advantages, perylene-based dyes are widely used as optical coloring materials for displays among many other useful applications [5-11]. Moreover, perylene dyes are easily functionalized through the introduction of substituents at their terminal- and bay-positions, which enables the modification of characteristics such as their spectral properties and solubilities [12-14]. Perylene diimide derivatives having two bulky substituents at their terminal-positions are commonly used, and these molecules are often modified for various purposes by the introduction of 1–4 substituents at their bay-positions.

Previously, we have reported many novel perylene-based dyes for use as the red colorants in LCD color filters [7,8,12-22]. Since the fluorescence of these dyes can negatively affect the optical performance of the color filters fabricated with them [21], we have also suggested solutions for this problem, in which the decrease of contrast ratios of color filters was inhibited by using perylene-based dyes with high solubility and low fluorescence [22]. Based on our previous reports, the effect of methoxy groups on the fluorescence properties of perylene-based dyes and the relationships between the fluorescence of the dyes and the position of the introduced methoxy groups are studied in this paper, both experimentally and theoretically.

In this study, perylene-based dyes which contained methoxy groups in the terminal-, bay-, or both positions were synthesized. The methoxy groups were sequentially placed at the *ortho*-, *meta*-, or *para*-position of each substituent. Additionally, the dyes with ethyl substituents instead of methoxy groups were designed and synthesized, these dyes have similar geometrical molecular structures and conjugation systems with the dyes containing methoxy groups [22]. The absorption and fluorescence properties of the synthesized dyes were measured and compared. The geometrical structures of the dyes were analyzed by density functional theory (DFT) calculations, and excitations from the highest occupied molecular orbitals (HOMOs) to the lowest

occupied molecular orbitals (LUMOs) of the dyes were simulated with time-dependent density functional theory (TD-DFT) [23,24]. Using these methods, the influence of the position of the methoxy groups on the electrochemical and the fluorescence properties of the dyes were studied.

2. Experimental

2.1. Materials and instrumentation

Perylene-3,4,9,10-tetracarboxylic dianhydride, iodine, sulfuric acid, bromine, and acetic acid were purchased from Sigma-Aldrich, 2,6-diisopropylaniline, 2-methoxy-6-methylaniline, 4-methoxy-2-methylaniline, 4-methoxyphenol, 4-ethylphenol, 3-methoxyphenol, 3-ethylphenol, 2-methoxyphenol, and 2-ethylphenol were purchased from TCI. Potassium carbonate anhydrous, methylene chloride, and other chemical solvents were purchased from Samchun Pure Chemical. All chemicals were used without any additional purification.

Absorption spectra were measured using a Perkin Elmer Lambda 25 UV/Vis spectrophotometer. Fluorescence spectra and quantum yield data were measured on a Perkin Elmer LS 55 and a PTI Quanta Master 40 fluorescence spectrometer, respectively. Elemental Analysis (EA) was completed on a CE Instruments EA1112 analyzer. ^{1}H and ^{13}C Nuclear Magnetic Resonance (NMR) spectra were recorded on a Bruker Avance 500 spectrometer running at 500 MHz using chloroform-d as a solvent with TMS as an internal standard. Matrix Assisted Laser Desorption/Ionization Time of Flight (MALDI-TOF) mass spectra were recorded on an Applied Biosystems Voyager-DE STR Biospectrometry Workstation using α-cyano-4-hydroxycinnamic acid (CHCA) as a matrix.

2.2. Syntheses of the dyes

All synthetic procedures were carried out by following our previous reports [20-22]. The dyes **PI-4EP**, **PI-4ME**, **P2M-4EP**, and **P2M-4ME** were already reported in our previous report [22]. The specified name of the dyes **P2M-4EP** and **P2M-4ME** were PM-4EP and PM-4ME in the report, respectively. The syntheses of these dyes are repeated in this paper.

2.2.1. 1,7-Dibromoperylene-3,4,9,10-tetracarboxydiimide : *Bromination*

Perylene-3,4,9,10-tetracarboxylic dianhydride (32.00 g, 81.40 mmol), iodine (0.78 g, 3.04 mmol) and sulfuric acid (98 %, 450 mL) were mixed and stirred for 2 h at room temperature. The temperature of the mixture was raised to 80 □ and bromine (8.33 mL, 162.80 mmol) was added dropwise over 1 h. The resulting mixture allowed to react for 16 h as sealed, upon which time, it was cooled to room temperature and the remaining bromine gas was displaced by nitrogen gas. The mixture was slowly poured into 3 L of ice water and the crude precipitate formed was collected by suction filtration followed by washing several times with distilled water. The crude product was dried at 80 □ under reduced pressure and used in the next step without further purification. The crude product containing both mono- and di-bromoperylene derivatives was separated by column chromatography in next step, after introducing bulky substituents in the terminal-position to increase their solubilities.

2.2.2. N,N'-bis(R_1)-1,7-dibromoperylene-3,4,9,10-tetracarboxydiimide : *Terminal-position substitution*

Crude 1,7-dibromoperylene-3,4,9,10-tetracarboxydiimide (8.00 g, 14.55 mmol), R_1-NH_2 (45.00 mmol), acetic acid (4.60 mL) and N-methyl-2-pyrrolidone (NMP, 100 mL) were mixed and heated to 120 □ under

nitrogen atmosphere for 96 h. Water was added to the mixture and the resulting precipitate was collected by suction filtration. The crude product was washed with water and dried under reduced pressure. The crude product was purified by column chromatography in silica gel using CH_2Cl_2 as an eluent. Three bands were collected. The first band contained a small amount of tribrominated diimide, the second band contained the dibrominated diimide, and the third contained the monobrominated diimide. Detailed structural analysis was conducted after the next step. To obtain the **PI-series**, 2,6-diisopropylaniline was used as R_1-NH_2, to obtain **PM-series**, 2-methoxy-6-methylaniline was used and to obtain **P2M-series**, and 4-methoxy-2-methylaniline was used for **P4M-series**.

2.2.3. N,N'-Bis(R_1)-1,7-bis(R_2)-perylene-3,4,9,10-tetracarboxydiimide : *Bay-position substitution*

N,N'-bis(R_1)-1,7-dibromoperylene-3,4,9,10-tetracarboxydiimide (0.58 mmol) was mixed with anhydrous potassium carbonate (0.35 g, 2.54 mmol), R_2-OH (1.60 mmol) and NMP (60 mL). The mixture was heated at 40 □ under nitrogen and was stirred for 1.5 h. Thin layer chromatography (TLC) of the crude was repetitively performed during the reaction to check the progress. After the reaction, the mixture was cooled to room temperature, and then poured into HCl aqueous solution (400 mL, 5 %). The precipitate was collected by suction filtration, washed with water and dried under vacuum at 80 □. The crude product was purified by column chromatography in silica gel using CH_2Cl_2 as an eluent to obtain the products as red solids.

Yield : **PI-3EP** (74.4 %), **PI-3ME** (73.5 %), **PI-2EP** (67.6 %), **PI-2ME** (67.0 %), **P4M-4EP** (65.9 %), **P4M-4ME** (62.1 %)

2.3. Geometry optimization of the dyes

Density functional theory (DFT) and Time-dependent density functional theory (TD-DFT) calculations were carried out with the Gaussian 09 program package. We used the 6-311++G(d,p) Pople basis set for all elements and the conventional B3LYP exchange-correlation function. The intermolecular interactions were analyzed by examining the core twist angles and the size of substituents. Dihedral angles of perylene main body

were calculated by measuring the distortion angle of benzene ring in the center of perylene main body. Calculated lengths of substituents were indicated by measuring the longest lineal distance of the atoms in the substituents. The spaces of the substituents away from the plane of perylene back bone were assessed by measuring the inserted angle between the substituents and the plane.

3. Results and discussion

3.1. Design concept of the synthesized dyes

The synthetic route and molecular structures of the synthesized dyes are shown in **Scheme 1** and **Fig. 1**, respectively. Seven dyes containing methoxy groups and three without methoxy groups were synthesized. The methoxy group, a readily available organic substituent and powerful electron donor, usually inhibits fluorescence when introduced into organic coloring materials [22,25-28]. To observe the effects of methoxy groups incorporated into bay-substituents, dyes containing methoxy groups in the *ortho*-, *meta*-, or *para*-position of bay-position benzene rings were designed. For comparison, analogs with ethyl groups introduced in place of the methoxy groups were also designed. To observe the effects of methoxy groups on the terminal-substituents, *ortho*- or *para*-methoxylated aryl substituents were introduced at the terminal-substituents of the dyes. Finally, the dyes with the methoxylated terminal-substituents carried only *para*-methoxy- or *para*-ethyl-aryl groups as their bay-substituents.

All the dyes were designed to have similar conjugation lengths and steric bulkiness, to minimize differences in the spectral properties and intermolecular interactions. As is widely known, the most impactful principal factor influencing the fluorescence of organic coloring materials is quenching through intermolecular interactions [29-33]. If H-aggregation intensively occurs, the excited energy is significantly consumed via non-radiative decay accompanied by intermolecular energy transfer, and as a result, radiative decay processes such

as emission are inhibited [30,34-36]. Therefore, the dyes used in this study were designed to have similar geometrical structures and intermolecular interactions so that their fluorescence properties would be primarily dependent on their electrochemical properties rather than their physical molecular behaviors [22].

3.2. Geometry optimization of the synthesized dyes

The optimized geometries of the synthesized dyes obtained via DFT calculations are shown in **Fig. 2**. The images as observed from the normal to the perylene main body plane are presented in **Fig. 2**. All the designed dyes have similar molecular morphologies, despite the introduction of the various substituents. The size of a dye molecule and its substituents majorly influence the distance between molecules [20], which, in turn, affects intermolecular interactions and fluorescence properties.

The dihedral angle of the perylene main body and the calculated lengths of the introduced substituents are listed in **Table 1**. The dihedral angle of the perylene main body was measured on the benzene ring at the center of perylene backbone [20]. All the introduced substituents are symmetrically oriented at each substitution position, but the dye molecules are not three-dimensionally symmetric according to the DFT simulations [20]. Therefore, all values were measured for both sides of the molecules and the average values are provided in **Table 1**. The synthesized dyes exhibited similar values for the dihedral angle of the perylene main body, which principally determines its planarity. The difference in the dihedral angles among the dyes is within about 1°, except for **PI-2ME**, therefore, it can be assumed that the planarity of the dyes is generally analogous to each other. As can be observed in **Table 1**, the dihedral angle data of **PI-2ME** is slightly out of the tendency. Our guess is that an unexpected error occurred in the case of **PI-2ME**, because the molecular structure of **PI-2ME** dye is less stable than the other dyes owing to the close proximity of the branches of the bay-substituents and the perylene backbone. This would increase the interference factor, and as a result, an error would be observed in the DFT calculations.

The sizes of introduced substituents are similar. Commonly, the bay-substituents with methoxy groups are smaller than those bearing ethyl groups by ~0.2 Å, and the terminal-substituents with methoxy groups are smaller than those without methoxy groups by ~1.2 Å. Generally, bulky substituents that contain several alkyl groups or benzene rings are used to prevent the intermolecular interactions of perylene-based dyes [3,21,22,37-43]. From this point of view, the difference of the physical morphologies of the dyes used in this study would not have a significant influence on the molecular interactions or the fluorescence behaviors of them.

3.3. Absorption properties of the synthesized dyes

The absorption properties of the synthesized dyes are shown in **Fig. 3** and **Table 2**. The absorption properties of the dyes have been reported in our previous study were remeasured and the measured results under this research are provided [22]. As intended, the overall shapes of the absorption spectra are similar, owing to the similar conjugation lengths designed for the synthesized dyes.

The dyes with *ortho*- or *para*-methoxylated bay-substituents exhibit bathochromic shifts of ~4 nm due to the electron donating effects of the methoxy groups. In contrast, the dye with *meta*-methoxylated bay-substituents shows a hypsochromic shift compared to the analogous dye with ethylated bay-substituents. These phenomena result from the well-known electron donating ability of the introduced organic substituents [25-27,44-47]. The same tendency is observed when methoxy groups are introduced in the terminal-substituents. However, the effects of electron donation by the methoxy groups appear to be more powerful when these groups are incorporated in the bay-substituents than in the terminal-substituents. The dyes with methoxylated terminal-substituents exhibited bathochromic shifts of only ~2 nm compared to the dyes without methoxy groups in the terminal-substituents.

3.4. Fluorescence properties of the synthesized dyes

The fluorescence properties of the synthesized dyes are presented in **Fig. 4** and **Table 3**. All fluorescence properties except quantum yield were measured at an excitation wavelength corresponding to the wavelength of maximum absorption. The quantum yield was measured at an excitation wavelength of 480 nm. Similarly to the absorption properties, the fluorescence properties of the dyes that were reported in our previous study were remeasured for comparison with the new dyes in this study [22]. The optical image of the synthesized dyes in chloroform solutions are shown in **Fig. 5**. The images were photographed under 365 or 254 nm of UV light.

Among the ten synthesized compounds, dyes **PI-4ME**, **P2M-4ME**, and **P4M-4ME** show quenched fluorescence, with differences in quantum yield of ~20-fold from the highly fluorescent dyes. The dyes with low fluorescence all bear methoxy groups at the *para*-positions of the bay-substituents. Compounds with methoxy groups at the *ortho*- or *meta*-positions of the bay-substituents show no fluorescence quenching. The differences in the fluorescence of the highly fluorescent dyes appear less significant compared to the obvious influences of *para*-methoxy groups in the bay-substituents. As observed above, methoxy groups electronically affect the absorption properties of perylene-based dyes irrespective of their positions. However, only the methoxy groups at the *para*-position of the bay-substituents inhibit fluorescence. Thus, the electrochemical influence of the introduced substituents on the fluorescence properties is dependent on their positions.

Methoxy groups introduced into terminal-substituents exerted a weaker influence on the fluorescence of dyes. *Ortho*-methoxylated terminal-substituents showed no fluorescence quenching effects, and those were *para*-methoxylated exhibited limited effects on fluorescence quenching compared to the cases with methoxy-bearing bay-substituents. It is widely known that the terminal-substituents have no or little influence on the conjugation systems of perylene-based dyes [41-43,48]. Comprehensively judged with the results of this study, it would seem that the terminal-substituents exert a very weak influence on the electrochemical properties of the perylene-based dyes, especially on their spectral properties, and these effects are very minor compared to the

influences of bay-substituents. However, it is not reasonable to assume that the terminal-substituents have no relationship with the conjugation systems of the perylene-based dyes.

3.5. Molecular orbital modeling of the synthesized dyes

The TD-DFT simulation results for excitation from the HOMOs to the LUMOs of the synthesized dyes are presented in **Table 4**. For each dye, the excitation system with the highest oscillator strength among the theoretically possible excitation systems is presented [23,24,49]. The maximum theoretical absorption wavelength changes along with the electron donating effect of the introduced substituents, although the results are not perfectly correlated with the measured data. Similar to the results of the DFT calculations, the simulations of dyes with groups at the *ortho*-positions of the bay-substituents show slight errors due to structural instability and the increase of interference factors.

The HOMO and LUMO molecular orbital models of the **PI-4EP**, **PI-4ME**, **PI-3ME**, **PI-2ME**, **P2M-4ME**, and **P4M-4ME** dyes are illustrated in **Fig. 6–11**, respectively. The HOMO and LUMO states are based on the results presented in **Table 4**, with the highest oscillator strength for each dye. For each figure, images of the HOMO state are presented in the upper three panels, and those of the LUMO state are presented below. The images as observed from the direction of x (terminal-substituents), y (bay-substituents), or z (normal of perylene main body plane) axis are sequentially presented for each state. The molecular orbital models of all the dyes are presented in the *supplementary data* in larger format.

The **PI-4ME**, **P2M-4ME**, and **P4M-4ME** dyes show inhibited fluorescence and have methoxy groups in the *para*-positions of the bay-substituents. Dyes **PI-3ME** and **PI-2ME** exhibit strong fluorescence and have methoxy groups in the *meta*- and *ortho*-positions, respectively. In the HOMO states of the fluorescence quenched dyes, electron density is clearly visible on the methoxy groups at the *para*-positions of the bay-substituents. In contrast, electron density is not observed on the methoxy groups in either the HOMO or LUMO

states of the highly fluorescent dyes. Thus, the methoxy groups exert an electrochemical influence through electron donation when they can overlap with the conjugation system of the perylene main body, effectively resulting in a fluorescence quenching effect.

The structural angles between the methoxy groups introduced in the bay-substituents and the perylene main body are listed in **Table 5**. *Para*-methoxy groups in the bay-substituents are oriented at an angle of 27° with respect to the perylene backbone, whereas the angle of methoxy groups in the *meta*-position is ~59° and that of the *ortho*-position is ~75°. Since the average observed dihedral angle of the perylene main body is ~13°, it can be assumed that the structural estranged degrees of the methoxy groups in the *para*-position of the bay-substituents are only about 15° when the plane of the perylene main body is assumed as a curved face. Therefore, the possibility that the methoxy groups at the *para*-positions of the bay-substituents overlap with the conjugation system of the perylene main body would be much higher than those of methoxy groups at other positions [50,51]. As a result, it could be concluded that the methoxy groups differently influence fluorescence quenching, dependent on their introduced position.

4. Conclusion

In this study, the effects of methoxy groups on the fluorescence of perylene-based dyes were studied with dyes that contained methoxy groups in various positions. To observe the effects of the methoxy group at the bay-substituents, dyes bearing *ortho*-, *meta*-, or *para*-methoxybenzene groups as bay-substituents were designed. To observe the effects of the methoxy groups in the terminal-substituents, dyes with *ortho*- or *para*-methoxyaryl groups as terminal-substituents were designed. Additionally, dyes with ethyl groups introduced instead of methoxy groups were also designed for comparison.

The geometries of the dyes were analyzed by the DFT method to assure the similarity of their structural morphologies. The introduced methoxy groups show a significant relationship with the spectral properties of the dyes. In particular, methoxy groups incorporated in the bay-substituents exhibited a stronger influence than those in the terminal-substituents. Dyes with *para*-methoxylated bay-substituents showed significantly quenched fluorescence. These *para*-methoxy groups in the bay-substituents exhibit the smallest structural dihedral angle with respect to the perylene main body, and therefore, would easily contribute to the conjugation system and affect the electrochemical properties. According to the TD-DFT calculations, electron density is only exhibited on the methoxy groups at the *para*-positions of the bay-substituents in the HOMO states of fluorescence quenched dyes. In conclusion, the methoxy groups that can overlap with the conjugation plane of the perylene main body influence the electrochemical and fluorescence properties of the dyes.

Acknowledgements

This work was supported by the Technology Innovation Program (No. 10052798) funded By the Ministry of Trade, Industry & Energy (MI, Korea).

Reference

[1] Chao CC, Leung Mk. Photophysical and Electrochemical Properties of 1,7-Diaryl-Substituted Perylene Diimides. J Org Chem 2005;70:4323-31.

[2] Zhao C, Zhang Y, Renjie Li XL, Jiang J. Di(alkoxy)- and Di(alkylthio)-Substituted Perylene-3,4;9,10-tetracarboxy Diimides with Tunable Electrochemical and Photophysical Properties. J Org Chem 2006;72:2402-10.

[3] Dincalp H, Askar Z, Zafer C, Icli S. Effect of side chain substituents on the electron injection abilities of unsymmetrical perylene diimide dyes. Dyes Pigm 2011;91:182-91.

[4] Huang C, Barlow S, Marder SR. Perylene-3,4,9,10-tetracarboxylic acid diimides: synthesis, physical properties, and use in organic electronics. J Org Chem 2011;76:2386-407.

[5] Reghu RR, Bisoyi HK, Grazulevicius JV, Anjukandi P, Gaidelis V, Jankauskas V. Air stable electron-

transporting and ambipolar bay substituted perylene bisimides. J Mater Chem 2011;21:7811.

[6] Lee SK, Zu Y, Herrmann A, Geerts Y, Müllen K, Bard AJ. Electrochemistry, Spectroscopy and Electrogenerated Chemiluminescence of Perylene, Terrylene, and Quaterrylene Diimides in Aprotic Solution. J Am Chem Soc 1999;121:3513-20.

[7] Kim YD, Kim JP, Kwon OS, Cho IH. The synthesis and application of thermally stable dyes for ink-jet printed LCD color filters. Dyes Pigm 2009;81:45-52.

[8] Choi J, Kim SH, Lee W, Chang JB, Namgoong JW, Kim YH, et al. The influence of aggregation behavior of novel quinophthalone dyes on optical and thermal properties of LCD color filters. Dyes Pigm 2014;101:186-95.

[9] Biedermann F, Elmalem E, Ghosh I, Nau WM, Scherman OA. Strongly fluorescent, switchable perylene bis(diimide) host-guest complexes with cucurbit[8]uril in water. Angew Chem Int Ed 2012;51:7739-43.

[10] Stolarski R, Fiksinski KJ. Fluorescent perylene dyes for liquid crystal displays. Dyes Pigm 1994;24:295-303.

[11] Qiao Y, Chen J, Yi X, Duan W, Gao B, Wu Y. Highly fluorescent perylene dyes with large stokes shifts: synthesis, photophysical properties, and live cell imaging. Tetrahedron Lett 2015;56:2749-53.

[12] Choi J, Sakong C, Choi JH, Yoon C, Kim JP. Synthesis and characterization of some perylene dyes for dye-based LCD color filters. Dyes Pigm 2011;90:82-8.

[13] Kim YD, Cho JH, Park CR, Choi JH, Yoon C, Kim JP. Synthesis, application and investigation of structure–thermal stability relationships of thermally stable water-soluble azo naphthalene dyes for LCD red color filters. Dyes Pigm 2011;89:1-8.

[14] Sakong C, Kim YD, Choi JH, Yoon C, Kim JP. The synthesis of thermally-stable red dyes for LCD color filters and analysis of their aggregation and spectral properties. Dyes Pigm 2011;88:166-73.

[15] Choi J, Lee W, Sakong C, Yuk SB, Park JS, Kim JP. Facile synthesis and characterization of novel coronene chromophores and their application to LCD color filters. Dyes Pigm 2012;94:34-9.

[16] Choi J, Lee W, Namgoong JW, Kim TM, Kim JP. Synthesis and characterization of novel triazatetrabenzcorrole dyes for LCD color filter and black matrix. Dyes Pigm 2013;99:357-65.

[17] Kim SH, Choi J, Sakong C, Namgoong JW, Lee W, Kim DH, et al. The effect of the number, position, and shape of methoxy groups in triphenylamine donors on the performance of dye-sensitized solar cells. Dyes Pigm 2015;113:390-401.

[18] Kim SH, Namgoong JW, Yuk SB, Kim JY, Lee W, Yoon C, et al. Synthesis and characteristics of metal-phthalocyanines tetra-substituted at non-peripheral (α) or peripheral (β) positions, and their applications in LCD color filters. J Inclusion Phenom Macrocyclic Chem 2015;82:195-202.

[19] Yuk SB, Lee W, Namgoong JW, Choi J, Chang JB, Kim SH, et al. Synthesis and characterization of bay-substituted perylene dyes for LCD black matrix of low dielectric constant. J Inclusion Phenom Macrocyclic Chem 2015;82:187-94.

[20] Kim JY, Choi J, Namgoong JW, Kim SH, Sakong C, Yuk SB, et al. Synthesis and characterization of novel perylene dyes with new substituents at terminal-position as colorants for LCD color filter. J Inclusion Phenom Macrocyclic Chem 2015;82:203-12.

[21] Kim JY, Sakong C, Choi S, Jang H, Kim SH, Chang KS, et al. The Effect of Fluorescence of Perylene Red Dyes on the Contrast Ratio of LCD Color Filters. Dyes Pigm 2016;131:293-300.

[22] Kim JY, Hwang TG, Kim SH, Namgoong JW, Kim JE, Sakong C, et al. Synthesis of high-soluble and non-

fluorescent perylene derivatives and their effect on the contrast ratio of LCD color filters. Dyes Pigm 2017;136:836-45.

[23] Tretiak S. Triplet State Absorption in Carbon Nanotubes: A TD-DFT Study. Nano Lett 2007;7:2201-6.

[24] Li GY, Chu T. TD-DFT study on fluoride-sensing mechanism of 2-(2'-phenylureaphenyl)benzoxazole: the way to inhibit the ESIPT process. Phys Chem Chem Phys 2011;13:20766-71.

[25] Pu S, Fan C, Miao W, Liu G. The effect of substituent position upon unsymmetrical isomeric diarylethenes bearing a methoxy group. Dyes Pigm 2010;84:25-35.

[26] Saeed A, Shabir G. New fluorescent symmetrically substituted perylene-3,4,9,10-dianhydride-azohybrid dyes: Synthesis and spectroscopic studies. Spectrochim Acta A 2014;133:7-12.

[27] Suzuki R, Tada R, Miura Y, Yoshioka N. Synthesis and physicochemical properties of methoxy-substituted diphenyldihydroacridine and its Si and Ge bridged analogues and corresponding nitroxide radical derivatives. J Mol Struct 2016;1106:399-406.

[28] Korzdorfer T, Tretiak S, Kummel S. Fluorescence quenching in an organic donor-acceptor dyad: a first principles study. J Chem Phys 2009;131:034310.

[29] Andreussi O, Corni S, Mennucci B, Tomasi J. Radiative and nonradiative decay rates of a molecule close to a metal particle of complex shape. J Chem Phys 2004;121:10190-202.

[30] Kang J, Jung J, Kim SK. Flexibility of single-stranded DNA measured by single-molecule FRET. Biophys Chem 2014;195:49-52.

[31] Kim M, Park WB, Bang B, Kim CH, Sohn KS. Radiative and non-radiative decay rate of K2SiF6:Mn4+phosphors. J Mater Chem C 2015;3:5484-9.

[32] Kwon J, Hwang J, Park J, Han GR, Han KY, Kim SK. RESOLFT nanoscopy with photoswitchable organic fluorophores. Sci Rep 2015;5:17804.

[33] Mazurak Z, Wanic A, Karolczak J, Czaja M. The fluorescence decay times and quantum efficiencies of 1,4,5,8-naphthalisoimides. J Lumin 2015;158:103-9.

[34] Bae S, Lim E, Hwang D, Huh H, Kim SK. Torsion-dependent fluorescence switching of amyloid-binding dye NIAD-4. Chem Phys Lett 2015;633:109-13.

[35] Karolin J, Johansson LBA, Ring U, Langhals H. Aggregation of perylene dyes in lipid vesicles: The effect of optically active substituents. Spectrochim Acta A 1996;52:747-53.

[36] Wurthner F, Thalacker C, Diele S, Tschierske C. Fluorescent J-type Aggregates and Thermotropic Columnar Mesophases of Perylene Bisimide Dyes. Chem Eur J 2001;7:2245-53.

[37] Turkmen G, Erten-Ela S, Icli S. Highly soluble perylene dyes: Synthesis, photophysical and electrochemical characterizations. Dyes Pigm 2009;83:297-303.

[38] Gao B, Li H, Liu H, Zhang L, Bai Q, Ba X. Water-soluble and fluorescent dendritic perylene bisimides for live-cell imaging. Chem Commun 2011;47:3894-96.

[39] Osswald P, Wurthner F. Conformational Effects of Bay Substituents on Optical, Electrochemical and Dynamic Properties of Perylene Bisimides: Macrocyclic Derivatives as Effective Probes. Chem Eur J 2007;13:7395-409.

[40] Zhang X, Wu Y, Li J, Li F, Li M. Synthesis and characterization of perylene tetracarboxylic bisester monoimide derivatives. Dyes Pigm 2008;76:810-6.

[41] Georgiev NI, Sakr AR, Bojinov VB. Design and synthesis of novel fluorescence sensing perylene diimides

based on photoinduced electron transfer. Dyes Pigm 2011;91:332-9.

[42] Lee IL, Li SR, Chen KF, Ku PJ, Singh AS, Kuo HT, et al. Synthesis, Photophysical Properties, and Field-Effect Characteristics of (Ethynylphenyl)benzimidazole-Decorated Anthracene and Perylene Bisimide Derivatives. Eur J Org Chem 2012;15:2906-15.

[43] Tsai HY, Chen KY. Synthesis and optical properties of novel asymmetric perylene bisimides. J Lumin 2014;149:103-11.

[44] Hutchings MG. Unexpected Bathochromic Shifts in the Visible Absorption Spectra of Arylazo Dyes Containing the orfho-N-pyridinium-nitro Substituent Combination. Dyes Pigm 1991;17:227-40.

[45] Durbeej B, Eriksson LA. On the bathochromic shift of the absorption by astaxanthin in crustacyanin: a quantum chemical study. Chem Phys Lett 2003;375:30-8.

[46] Lakshmi Praveen P, Ojha DP. Effect of molecular interactions and end chain length on ultraviolet absorption behavior and photo stability of alkoxycinnamic acids: Theoretical models of liquid crystal. J Mol Liq 2014;197:106-13.

[47] Outlaw VK, Zhou J, Bragg AE, Townsend CA. Unusual blue-shifted acid-responsive photoluminescence behavior in 6-amino-8-cyanobenzo[1,2-b]indolizines. RSC Adv 2016;6:61249.

[48] Erdogmus A, Nyokong T. Novel, soluble, FluXoro functional substituted zinc phthalocyanines; synthesis, characterization and photophysicochemical properties. Dyes Pigm 2010;86:174-81.

[49] Zhou J, Outlaw VK, Townsend CA, Bragg AE. Quenching of pH-Responsive Luminescence of a Benzoindolizine Sensor by an Ultrafast Hydrogen Shift. Chem Eur J 2016;22:15212-5.

[50] Chen J, Shi MM, Hu XL, Wang M, Chen HZ. Conjugated polymers based on benzodithiophene and arylene imides: Extended absorptions and tunable electrochemical properties. Polymer 2010;51:2897-902.

[51] Dincalp H, Kizilok S, Icli S. Fluorescent macromolecular perylene diimides containing pyrene or indole units in bay positions. Dyes Pigm 2010;86:32-41.

Figure Captions

Fig. 1. Structure of the synthesized dyes.

Fig. 2. Geometry-optimized structure of the synthesized dyes.

Fig. 3. Absorption spectra of the synthesized dyes in chloroform (10^{-5} mol/L).

Fig. 4. Fluorescence spectra of the synthesized dyes in chloroform (10^{-8} mol/L).

Fig. 5. Optical image of the synthesized dyes in chloroform solutions (10^{-4} mol/L) under UV light of (a) 365 nm and (b) 254 nm.

Fig. 6. Molecular orbital model of **PI-4EP** at HOMO and LUMO.

Fig. 7. Molecular orbital model of **PI-4ME** at HOMO and LUMO.

Fig. 8. Molecular orbital model of **PI-3ME** at HOMO and LUMO.

Fig. 9. Molecular orbital model of **PI-2ME** at HOMO and LUMO.

Fig. 10. Molecular orbital model of **P2M-4ME** at HOMO and LUMO.

Fig. 11. Molecular orbital model of **P4M-4ME** at HOMO and LUMO.

Table 1 Dihedral angles of the perylene main body and calculated lengths of the substituents. [a]

Dye	Dihedral angle of the perylene main body (°)	Calculated lengths of substituents (Å)	
		Bay-substituent	Terminal-substituent
PI-4EP	13.66954	7.61265	8.91653
PI-4ME	13.65821	7.39409	8.91467
PI-3EP	12.70249	7.22121	8.83280
PI-3ME	12.90190	7.10929	8.90940
PI-2EP	12.82097	7.23594	8.82305
PI-2ME	13.89031	7.11218	8.90961
P2M-4EP	13.58233	7.61336	7.76763
P2M-4ME	13.65405	7.39385	7.76759
P4M-4EP	13.18395	7.50709	7.56291
P4M-4ME	13.57888	7.39411	7.56386

[a] dihedral angle and calculated lengths are not symmetric for each side of perylene main body, therefore, the average values are listed.

Table 2 Spectral properties of the synthesized dyes.

Dye	λ_{abs} [a]	ε_{abs} [b]
PI-4EP	546	62,050
PI-4ME	550	56,650
PI-3EP	544	59,880
PI-3ME	540	54,940
PI-2EP	550	61,520
PI-2ME	554	70,520
P2M-4EP	548	56,510
P2M-4ME	552	60,000
P4M-4EP	548	55,040
P4M-4ME	552	51,940

[a] λ_{abs} : maximum absorption wavelength (nm).

[b] ε_{abs} : molar extinction coefficient (L/mol·cm).

Table 3 Fluorescence properties of the synthesized dyes.

Dye	λ_{em} [a]	Maximum emission intensity (a.u.)	Q_y [b]
PI-4EP	581	241.82	0.976
PI-4ME	586	7.08	0.054
PI-3EP	578	241.62	0.938
PI-3ME	576	227.61	0.926
PI-2EP	579	256.49	0.947
PI-2ME	582	242.51	0.961
P2M-4EP	580	226.75	0.985
P2M-4ME	582	10.20	0.080
P4M-4EP	580	215.44	0.880
P4M-4ME	584	6.38	0.040

[a] λ_{em} : maximum emission wavelength (nm).

[b] Q_y : quantum yield (10^{-5} mol/L in chloroform, excited at 480 nm).

Table 4 Calculated result of TD-DFT for the excitation from HOMO to LUMO of the synthesized dyes.

Dye	Definition	Transition	Excitation energy (eV)	Theoritical λ_{abs} (nm)	Oscillator strength
PI-4EP	252 → 253	$S_0 \rightarrow S_1$	2.2911	541.15	0.7918
PI-4ME	252 → 253	$S_0 \rightarrow S_1$	2.2661	547.13	0.7547
PI-3EP	252 → 253	$S_0 \rightarrow S_1$	2.2710	545.95	0.7629
PI-3ME	252 → 253	$S_0 \rightarrow S_1$	2.2861	542.34	0.7632
PI-2EP	252 → 253	$S_0 \rightarrow S_1$	1.8731	661.91	0.7067
PI-2ME	252 → 253	$S_0 \rightarrow S_1$	2.2541	550.04	0.7775
P2M-4EP	228 → 229	$S_0 \rightarrow S_1$	2.3215	534.06	0.7583
P2M-4ME	228 → 229	$S_0 \rightarrow S_1$	2.2951	540.20	0.7268
P4M-4EP	228 → 229	$S_0 \rightarrow S_1$	2.2817	543.38	0.7525
P4M-4ME	228 → 229	$S_0 \rightarrow S_1$	2.2846	542.69	0.7405

Table 5 Structural angle between the methoxy group at bay-substituents and the plane of perylene main body.

Dye	PI-4ME	PI-3ME	PI-2ME	P2M-4ME	P4M-4ME
Angle (°)	26.287	58.863	74.911	28.109	27.657

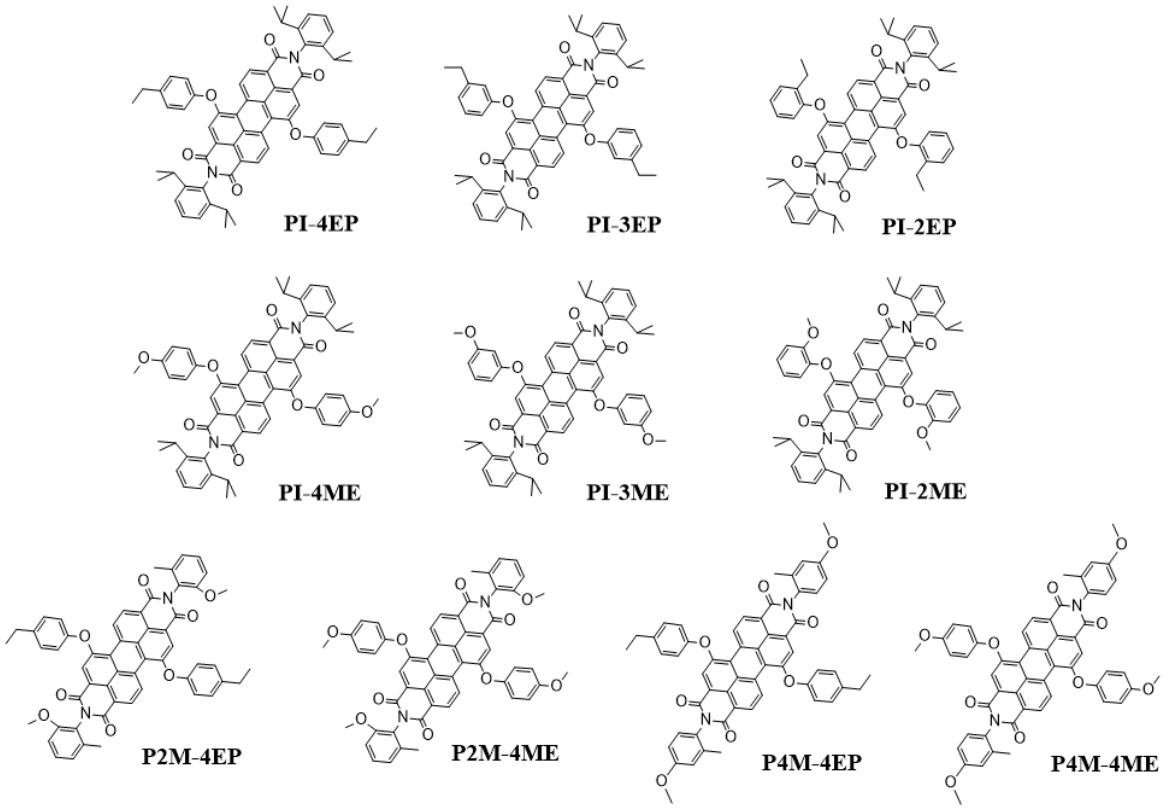

Fig. 1. Structure of the synthesized dyes.

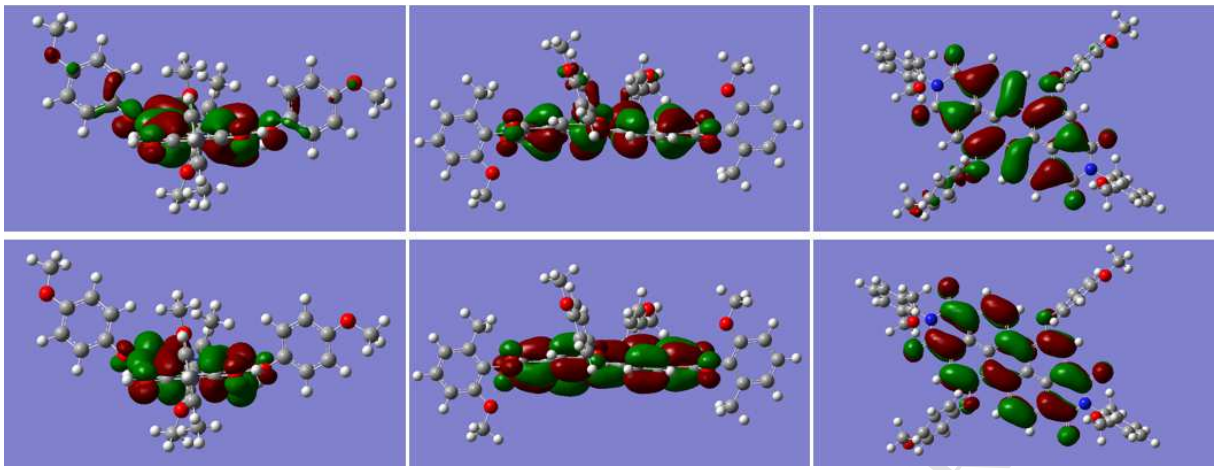

Fig. 10. Molecular orbital model of **P2M-4ME** at HOMO and LUMO.

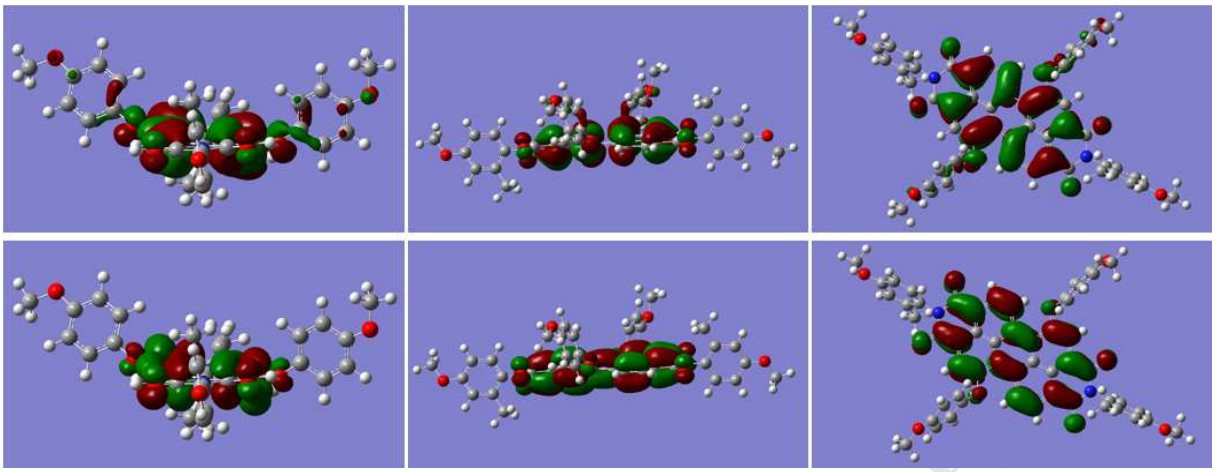

Fig. 11. Molecular orbital model of **P4M-4ME** at HOMO and LUMO.

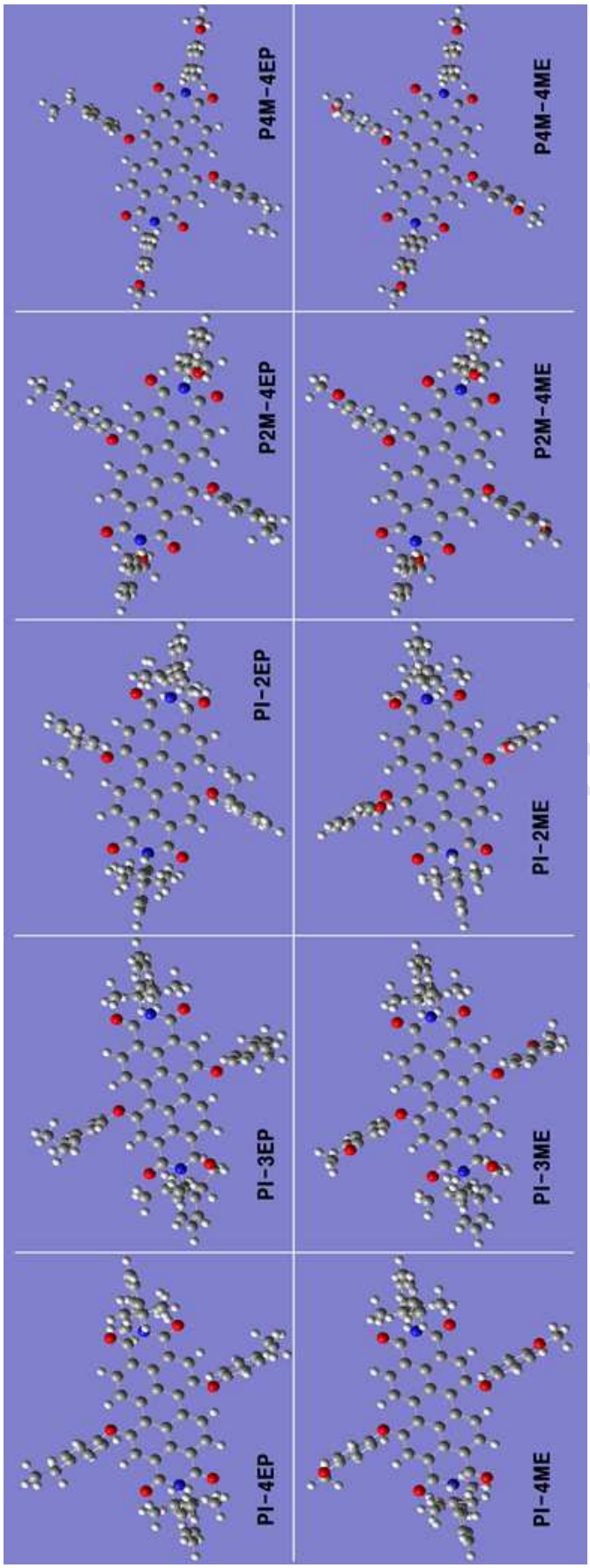

Fig. 2. Geometry-optimized structure of the synthesized dyes.

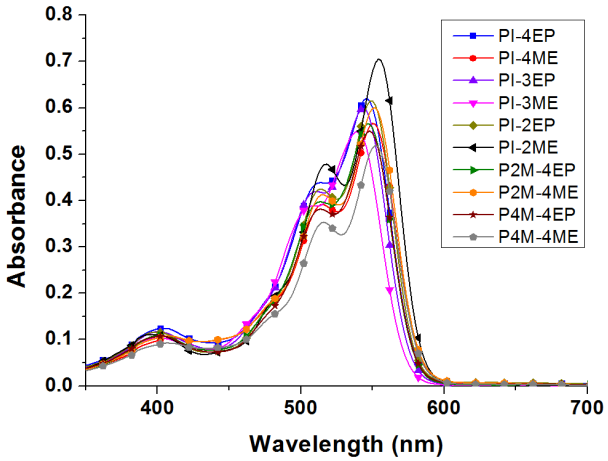

Fig. 3. Absorption spectra of the synthesized dyes in chloroform (10^{-5} mol/L).

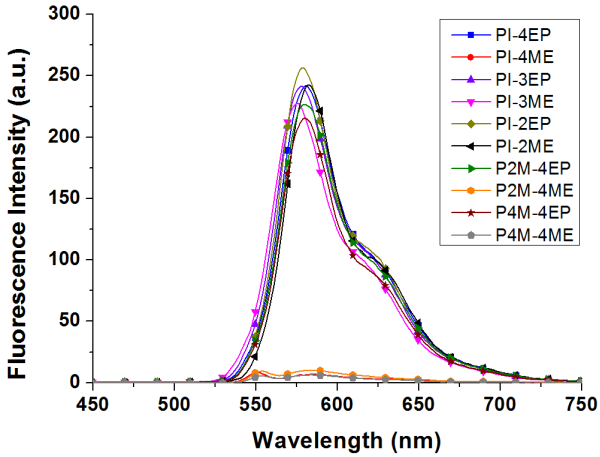

Fig. 4. Fluorescence spectra of the synthesized dyes in chloroform (10^{-8} mol/L).

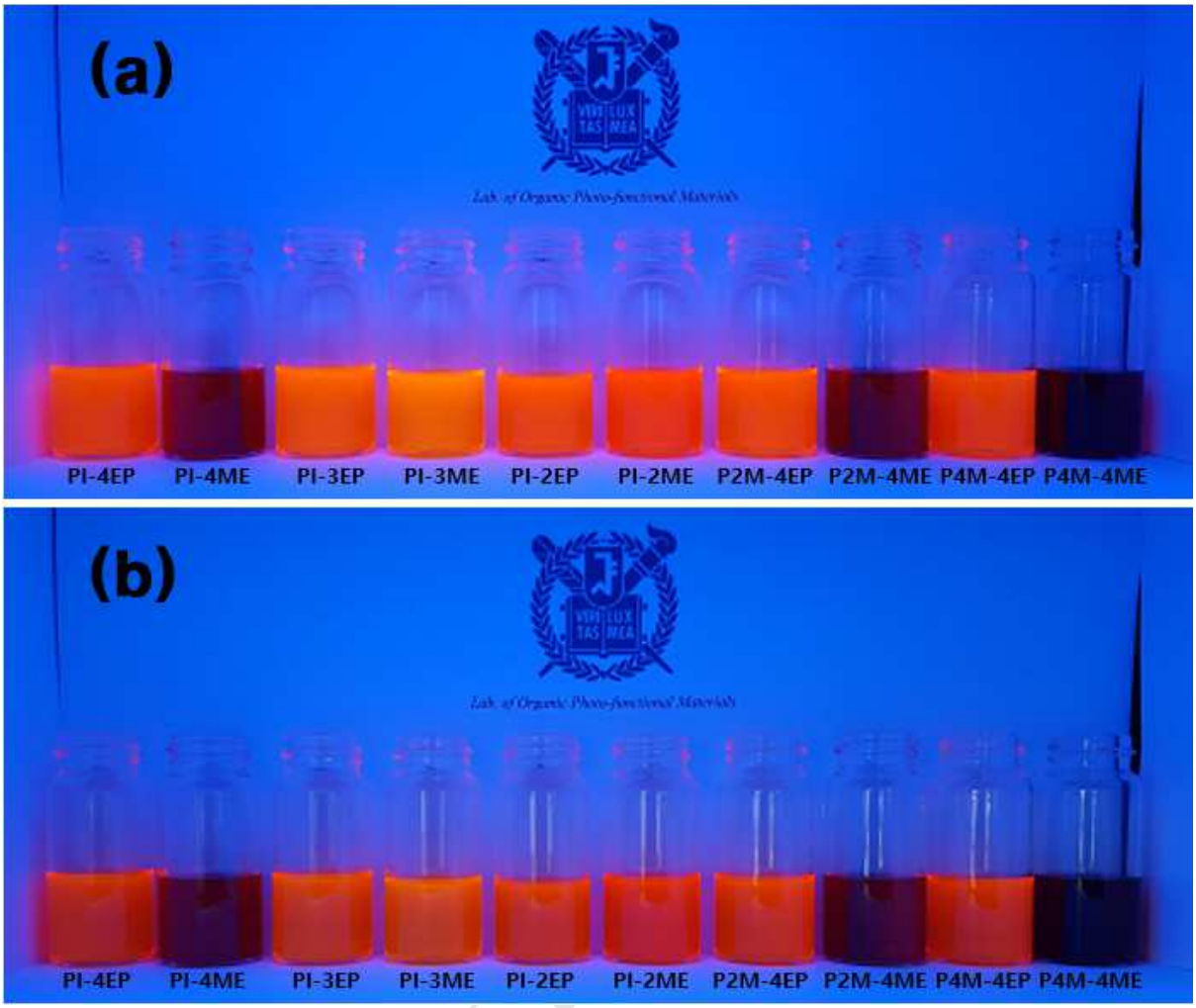

Fig. 5. Optical image of the synthesized dyes in chloroform solutions (10^{-4} mol/L) under UV light of (a) 365 nm and (b) 254 nm.

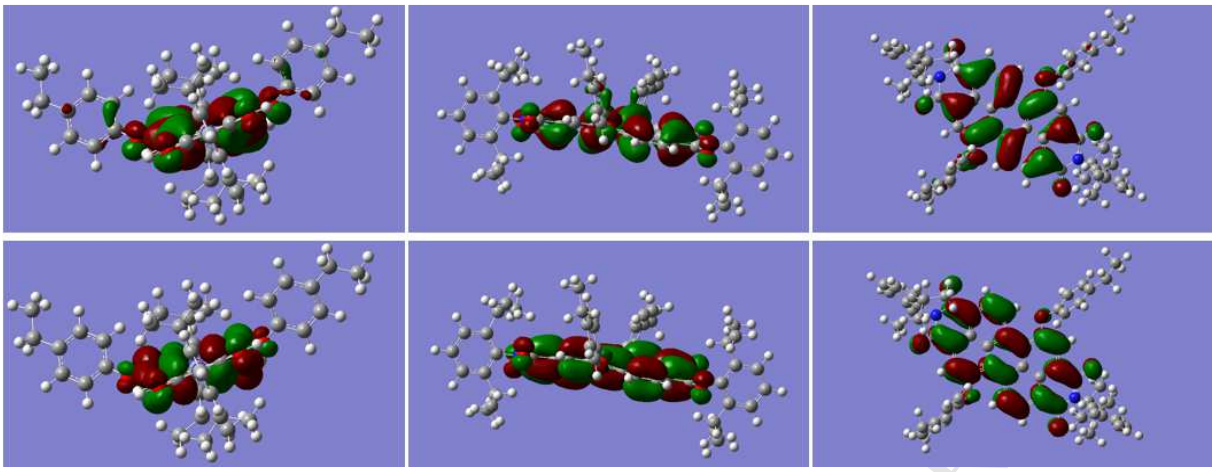

Fig. 6. Molecular orbital model of **PI-4EP** at HOMO and LUMO.

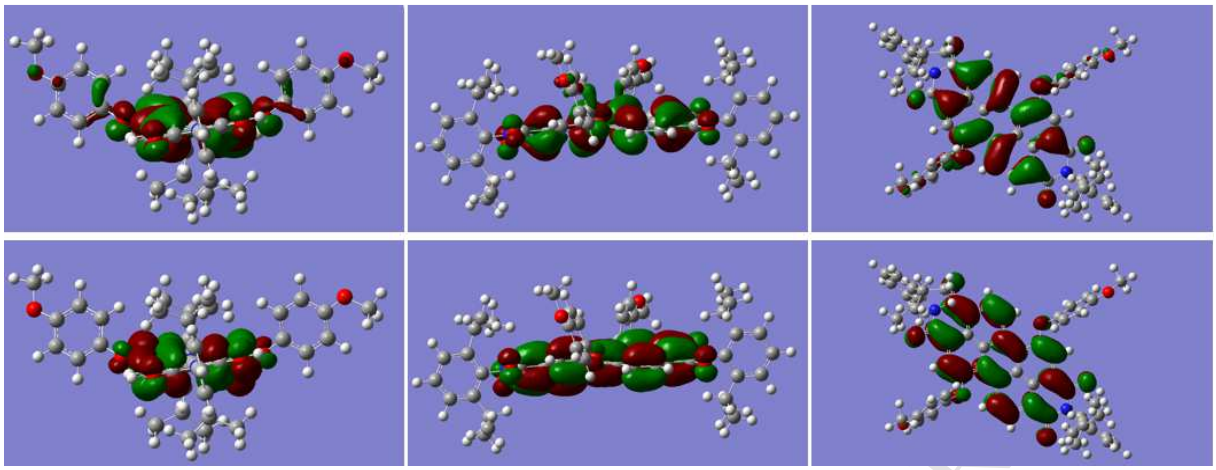

Fig. 7. Molecular orbital model of **PI-4ME** at HOMO and LUMO.

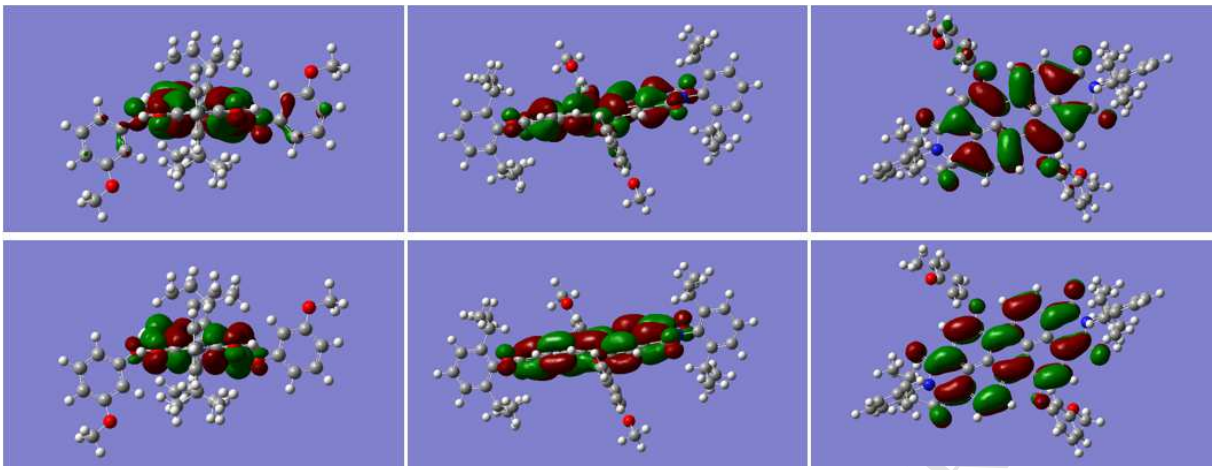

Fig. 8. Molecular orbital model of **PI-3ME** at HOMO and LUMO.

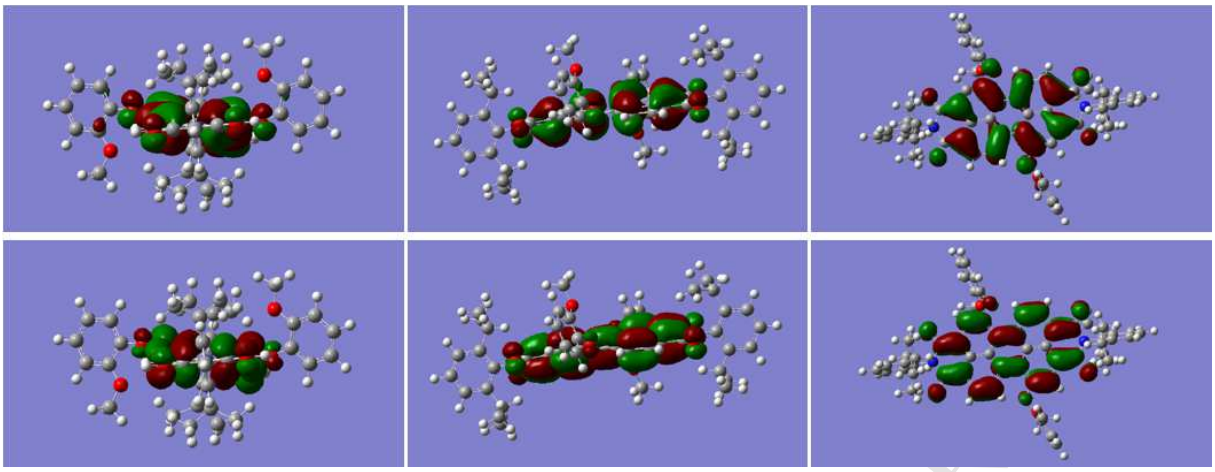

Fig. 9. Molecular orbital model of **PI-2ME** at HOMO and LUMO.

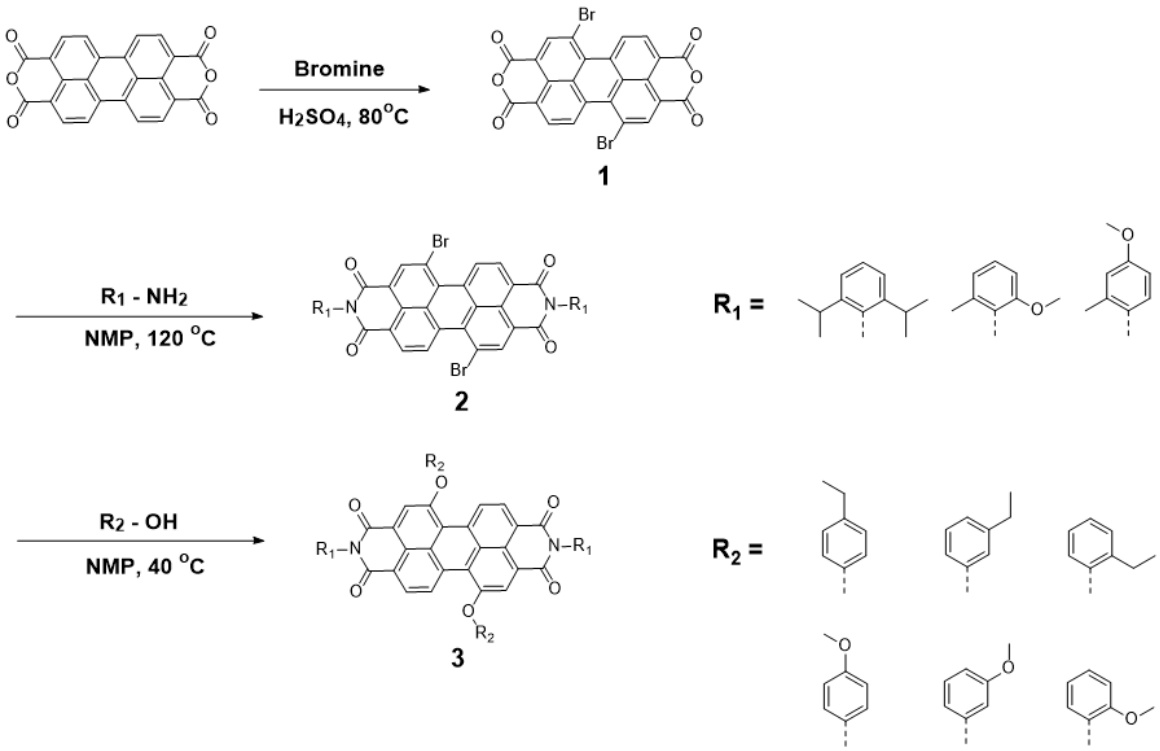

Scheme 1. Synthetic routes of the designed dyes.

Highlights

Perylene-based dyes with methoxy groups at various positions are synthesized.

Absorption, fluorescence properties and TD-DFT simulations of the dyes are studied.

Only the methoxy groups at the para-position of bay-substituents inhibit the fluorescence of dyes.

The methoxy groups have to be involved in the conjugation system of the dyes for the fluorescence quenching.